https://doi.org/10.1007/s11740-018-0813-4

Cutting force model for machining of CFRP laminatewith diamond abrasive cutter

A. Boudelier[1,2] · M. Ritou[1] · S. Garnier[1] · B. Furet[1]

Abstract
The article presents a cutting force model for trimming operations of CFRP laminate with diamond abrasive cutters. Those tools are more and more encountered on industrial applications of CFRP trimming, due to their abrasion resistance and their low cost. Contrary to endmills, they consist of a large number of cutting grits, randomly distributed around the tool. To tackle the issue, a continuous model of tool engagement is proposed. Validity of the approach is verified. A mechanical model of cutting forces, adapted to CFRP laminate, is then presented. The evolution of specific cutting coefficient in relation to fibres orientation is investigated through a piecewise constant model. It leads to the proposal of a sine model for the specific cutting coefficients. The simulated forces are in good agreement with the experimental results of cutting tests, carried out in multidirectional CFRP laminate for different fibres orientation and widths of cut. Cutting mechanisms are finally discussed depending on fibres orientation.

Keywords Cutting force model · Composite · Trimming · Multidirectional CFRP laminate · Diamond abrasive cutter · Cutting mechanism

1 Introduction

Machining of composite laminates is often difficult because of their mechanical and thermal properties: heterogeneity, anisotropy and low thermal conductivity [18]. Moreover, their high abrasiveness, notably mentioned by Ramkumar et al. [13] in drilling operations and Dumas et al. [7] in milling operations, conducts to premature tool wear. That is why diamond abrasive cutters, constituted of small diamond grits (Fig. 1), have been specifically developed for CFRP trimming operations. In comparison with carbide or polycrystalline diamond tools (PCD), tool life and productivity are improved while material integrity is respected. Moreover, costs are reduced.

Very few studies concern diamond abrasive cutters. Collingan and Ramulu [6] characterised trimmed surfaces depending on tool grits size and feedrate. They also performed preliminary tests to study influence of these parameters on cutting forces. Boudelier et al. [5] studied the CFRP machinability with diamond abrasive cutters. However, no cutting force model has been proposed for this tool technology whereas it is necessary in order to optimize cutting conditions and avoid material integrity defects.

Slamani et al. [15] studied the cutting force during the robotized trimming of CFRP. Force models have been proposed for orthogonal cutting with carbide [2] and PCD tools Wang et al. [12, 19]. Influence of fibres orientation, feed rate and cutting speed has essentially been studied. Empirical [20], numerical [1, 10, 14] and analytical models have been developed. The latter are based on a tangential—radial cutting force approach. At a macroscopic scale, the influence of fibres orientation can be integrated into the specific cutting coefficients through sine [3, 8, 16] or polynomial models [17]. At a microscopic scale, approaches based on the chip formation were developed, considering fibres breaking mechanisms [2, 11, 22]. Also, Yuan [21] proposed a force model for the ultrasonic machining of CFRP.

In this paper, an analytical model of cutting force for trimming operations of multidirectionnal CFRP laminate with diamond abrasive cutters is presented. Contrary to endmills, diamond cutters consist of a multitude of grits with

✉ M. Ritou
mathieu.ritou@univ-nantes.fr

[1] LS2N (Laboratory of Digital Sciences of Nantes, UMR CNRS 6004), Universite de Nantes, 44035 Nantes, France

[2] Laboratoire Arts et Metiers ParisTech d'Angers (LAMPA), Arts et Metiers ParisTech, Angers, France

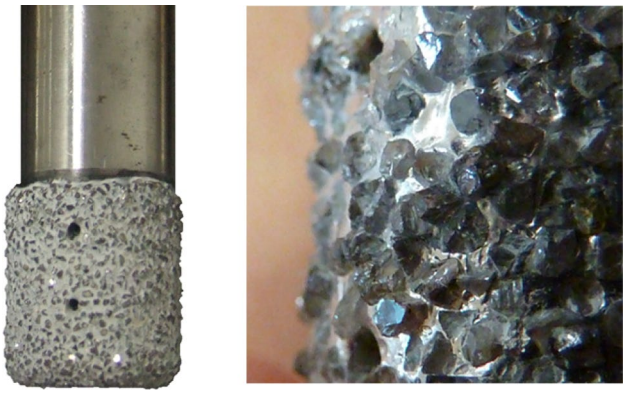

Fig. 1 Diamond abrasive cutter with grits size of 852 µm

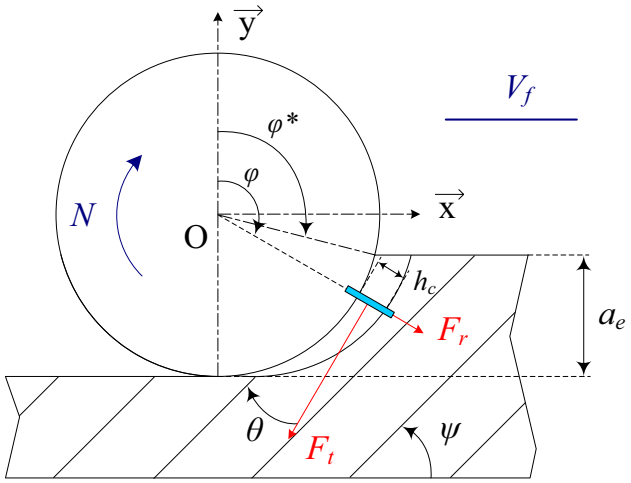

Fig. 2 Cutting forces at the cutting edge

irregular shapes that are randomly distributed around the tool [9]. That is why a continuous model of tool engagement is proposed. Secondly, as the influence of fibres orientation on the specific cutting coefficients is unknown, a first investigation is carried out based on a piecewise constant model. The results lead to the proposition of a sine model of specific cutting coefficients. Then, accuracy of the model is evaluated and compared to experiments carried out over the entire range of fibres orientation (− 90° to +90°). Finally, results of the model are expressed in the fibres reference system in order to discuss cutting mechanisms depending on fibres orientation.

2 Tool engagement models

2.1 Cutting edge model

Classical milling cutters rely on a given number of cutting edges. Tool engagement is modelled by localized engagements of cutting edges. Then, cutting forces generated by each cutting edge during material removal are proportional to chip thickness. Tangential and radial forces, applied by tool on material, are respectively defined by the following expressions:

$$\begin{aligned} F_t(\varphi) &= K_t(\theta) \cdot f_z \cdot \sin(\varphi).a_p \\ F_r(\varphi) &= K_r(\theta) \cdot f_z \cdot \sin(\varphi).a_p \end{aligned} \quad (1)$$

where K_t and K_r are the tangential and radial specific cutting coefficients (MPa), f_z is the feed per tooth (mm/rev/tooth), a_p the depth of cut (mm), φ the tooth angular position.

In the case of machining of CFRP laminates, the specific cutting coefficients vary with fibre orientation θ that corresponds to the angle between cutting speed direction and fibre orientation of the considered unidirectional ply in the laminate (Fig. 2). During tool revolutions, it evolves with the tool angular position.

2.2 Continuous model of tool engagement

Considering trimming operations with diamond abrasive cutters, cutting models must be adapted. Indeed, a diamond abrasive cutter is close to a grinding tool but with a larger grit size. Contrary to tools with cutting edges, it relies on a large number of grits, with a random distribution of height and position around the tool body (Fig. 1). From one tool to another, the distribution is different. Contrary to endmills, multiplicity and randomness of cutting grits lead to constant cutting forces during machining. Consequently, the classical approach with a localized engagement of each cutting edge is not appropriated.

The assumption is made that the grits distribution around the tool is homogenous and uniform. This is the reason why a continuous tool engagement model is proposed in the paper. At each instant, it is considered that the diamond abrasive cutter generates cutting forces all along the tool engagement domain. The domain is discretized into elementary sectors $d\chi$ (Fig. 3). In order to obtain the elementary tangential $F_{te}(\chi)$ and radial $F_{re}(\chi)$ forces for each elementary sector $d\chi$, angular specific cutting coefficients $K_t(\theta)/2\pi$ and $K_r(\theta)/2\pi$ must be introduced:

$$\begin{aligned} F_{te}(\chi) &= \frac{K_t(\theta)}{2 \cdot \pi} \cdot f \cdot a_p \cdot \sin(\chi) \\ F_{re}(\chi) &= \frac{K_r(\theta)}{2 \cdot \pi} \cdot f \cdot a_p \cdot \sin(\chi) \end{aligned} \quad (2)$$

where f is the feed per revolution (mm/rev).

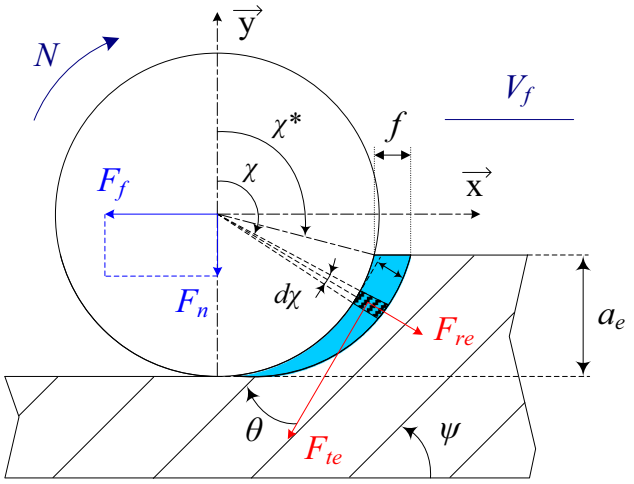

Fig. 3 Elementary cutting forces applied on a dχ sector

2.3 Coherence between the two approaches

The objective of the paragraph is to demonstrate that $K_t(\theta)$, which has been introduced in the expression of elementary tangential force with diamond abrasive cutter approach (Eq. 2), is similar to the one considered with endmills (Eq. 1). To do so, the mechanical works of the spindle during a revolution are compared for the two tool engagement approaches.

In case of machining with endmills, the spindle work W_c during one tool revolution is the sum of the work of each cutting edge j. It can be obtained by summing the instantaneous spindle power during one tool revolution period:

$$W_{c=} \sum_{j=1}^{Z} \int_{0}^{T} V_c \cdot F_t \cdot dt \tag{3}$$

where T is the tool revolution period, V_c the tool cutting speed and R the tool radius. Considering that $V_c = R.d\varphi/dt$, and introducing Eq. [1] in (3), the spindle work can be expressed as:

$$W_c = R \cdot f \cdot a_p \cdot \int_{\varphi*}^{\pi} K_t(\theta) \cdot \sin(\varphi) \cdot d\varphi \tag{4}$$

In case of machining with diamond abrasive cutter, the instantaneous spindle power P_d resulting from the elementary tangential forces $F_{te}(\chi)$ can be expressed as:

$$P_d = \int_{\chi*}^{\pi} V_c \cdot F_{te}(\chi) \cdot d\chi \tag{5}$$

From Eq. [2], it follows that:

$$P_d = V_c \cdot f \cdot a_p \cdot \int_{\chi*}^{\pi} \frac{K_t(\theta)}{2.\pi} \cdot \sin(\chi) \cdot d\chi \tag{6}$$

As the tool is considered as continuously engaged (Fig. 3), the spindle power is constant. Thus, the spindle work for abrasive cutter W_d is simply given by:

$$W_d = \int_{0}^{T} P_d \cdot dt = P_d \cdot T \tag{7}$$

As the period $T = 2\pi R/V_c$, the work can be written as:

$$W_d = R \cdot f \cdot a_p \int_{\chi*}^{\pi} K_t(\theta) \cdot \sin(\chi) \cdot d\chi \tag{8}$$

The analytical expressions of the spindle work (Eqs. 4 and 8) are identical for the two tool engagement models. Consequently, the specific cutting coefficients that will be identified in the paper can be compared with ones obtained for other cutting tool technologies.

3 Cutting force model for multidirectional laminate

The CFRP multidirectional laminates of aeronautic structure consist in a stack of plies with, generally, unidirectional carbon fibres (see Fig. 4); according to the laminate lay-up that defines the sequence of ply orientations (see lay-up in Table 1). ψ represents the fibre orientation of a given ply, in relation to feed direction.

Let's consider the machining of a given ply with a diamond abrasive cutter, the local depth of cut corresponds to the ply thickness e. The feed force $F_f(\psi)$ and the normal force $F_n(\psi)$ can be obtained by summing the elementary forces along the tool engagement domain. After projection in the feed reference system (x,y), they can be expressed by the following expressions:

$$\begin{bmatrix} F_f(\psi) \\ F_n(\psi) \end{bmatrix} = \frac{f}{2.\pi} \cdot e \cdot \int_{\chi*}^{\pi} \sin(\chi) \cdot \begin{bmatrix} \cos\chi & \sin\chi \\ -\sin\chi & \cos\chi \end{bmatrix} \cdot \begin{bmatrix} K_t(\theta) \\ K_r(\theta) \end{bmatrix} \cdot d\chi \tag{9}$$

where ψ represents the fibre orientation in relation to feed direction. θ is the relative orientation between fibre and cutting direction:

$$\theta = \psi + \chi \quad \theta \in \left]-\pi/2;\pi/2\right] \tag{10}$$

In order to determine the average cutting forces generated during the trimming of a multidirectional laminate, a mixture approach is used [16, 1720]. It assumes that the

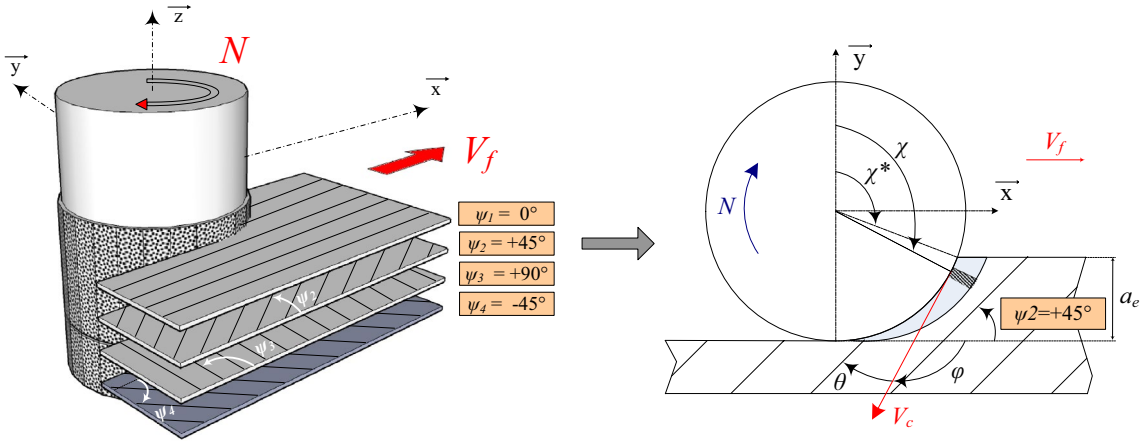

Fig. 4 Example of configuration of a multidirectional laminate, composed of m = 4 plies with unidirectional fibres

Table 1 Mechanical properties of carbon/epoxy material T800-M21 (Hexcel)

Number of plies	37
Ply thickness	0.27 mm
Fibre volume fraction	56.6%
Laminate Density	1580 kg/m^3
Compression modulus	136 GPa
Tensile modulus	172 GPa
Lay up	(90/− 45/0/45/0/45/0/− 45/0/0/0/0/− 45/90/90/45/0/90/ 90/0/45/90/− 45/90/− 45/0/0/0/0/− 45/0/45/0/45/0/− 45/90)

interactions between plies are neglected. Indeed, the interface between two plies is only composed of polymer matrix. Its mechanical behaviour during trimming is negligible in comparison with plies one's. This hypothesis will be validated in a following section. Consequently, the cutting forces can be simply obtained by summing the forces necessary to machine each unidirectional ply of the laminate (Fig. 4):

$$\begin{bmatrix} F_f \\ F_n \end{bmatrix} = \frac{f}{2 \cdot \pi} \cdot \sum_{i=1}^{m} n_{\psi_i} \cdot e_i \cdot \int_{\chi*}^{\pi} \sin(\chi) \cdot \begin{bmatrix} \cos\chi & \sin\chi \\ -\sin\chi & \cos\chi \end{bmatrix} \cdot \begin{bmatrix} K_t(\theta) \\ K_r(\theta) \end{bmatrix} \cdot d\chi \quad (11)$$

where m is the number of different ply orientations, $n_{\psi i}$ the number of ply oriented at an angle of ψ_i degrees and e_i the ply thickness, for a given orientation i.

4 Model of specific cutting coefficients

At this step of the study, the evolution of the specific cutting coefficients in relation to the relative fibre orientation θ is unknown. This is the reason why the expression of $K_t(\theta)$ and $K_r(\theta)$ are, in a first approach, modelled by a piecewise constant function in order to observe their evolution.

4.1 Investigation of the influence of fibres orientation on specific cutting coefficients

The relative fibre orientation θ varies from $-\pi/2$ to $+\pi/2$. It is divided into n_z different sectors of β_z degrees. The specific cutting coefficients $K_t(\theta)$ and $K_r(\theta)$ are assumed constant for each sector. As the feed direction and the ply orientation ψ remain identical during the cutting tests, the relative fibre orientation θ also remains identical considering a given sector of the tool (Fig. 5).

Consequently, the tangential and radial specific cutting coefficients are considered constant for each sector of the tool. Hence, only tool sectors will be considered. In this way, the feed force can be expressed as:

$$F_f = \frac{f}{2.\pi} \cdot \sum_{i=1}^{m} n_{\psi i} \cdot e_i \cdot \left[\sum_{j=n_{ze}}^{n_z} K_t(\theta_{ij}) \cdot \int_{(j-1)\cdot\beta_z}^{j\cdot\beta_z} \sin(\chi) \cdot \cos(\chi) \cdot d\chi + \sum_{j=n_{ze}}^{n_z} K_r(\theta_{ij}) \cdot \int_{(j-1)\cdot\beta_z}^{j\cdot\beta_z} \sin^2(\chi) \cdot d\chi \right] \quad (12)$$

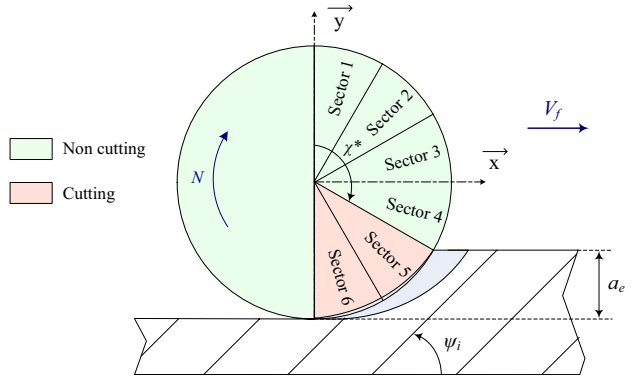

Fig. 5 Piecewise constant model

where θ_{ij} is the relative fibre orientation of an angular sector j, for a ply orientation i; and n_{ze} is the index of the first cutting sector of the tool, evaluated by the floor function of $n_z.\chi^*/\pi + 1$.

In this way, the Feed and Normal force models lead to a linear combination of the specific cutting coefficients, which will simplify their identification. Since the radial and tangential specific cutting coefficients are represented by a piecewise constant function, Eq. [12] can be expressed as a matrix product of the specific cutting coefficients K:

$$F = A.K \quad with \quad F = \begin{bmatrix} F_f \\ F_n \end{bmatrix}_{2n_{cut},1}, \quad K = \begin{bmatrix} K_t \\ K_r \end{bmatrix}_{2n_z,1} \quad and \quad A_{2n_{cut},2n_z} \tag{13}$$

where n_{cut} is the number of cutting tests. Therefore, the specific cutting coefficients can be identified by matrix inversion: $\mathrm{K} = \mathrm{A}^{-1}.\mathrm{F}$.

4.2 Experimental setup

An aeronautic CFRP laminate of T800-M21 was trimmed to carry out the experiments. The laminate was composed of 37 plies of unidirectional graphite fibre fabric, made by alternating four fibres orientations (Table 1). The matrix used was a thermosetting epoxy resin M21.

The diamond abrasive cutter used during the experiments was composed of natural diamond grits fixed with a nickel bond on a cylindrical body by electro deposition (Fig. 1). A 16 mm tool diameter with 852 µm grits size was used. Widths of cut of 16 mm (slot) and 5.94 mm (in down-milling) were machined. For a discretization of the tool engagement in 12 sectors (n_z=12) in the piecewise model (Fig. 5), these two widths of cut have solicited respectively 12 (χ^*=0°) or 5 tool sectors (χ^*=105°). For each width of cut, 12 machining directions from ψ=0° to 180° were studied.

Trimming tests were carried out on a three-axis Huron KX30 milling machine, equipped with a 28,000 RPM −40 kW Kessler spindle. Cutting forces were measured using a 9255B Kistler three-component dynamometer. It was mounted between the workpiece and the table of the machining centre. Contrary to endmills, diamond abrasive cutters lead to constant cutting forces during cuts. So, for each run, average values of feed force F_f and normal force F_n are evaluated and resultant of cutting forces F is calculated.

Table 2 Cutting conditions

Cutting speed	1400 m/min
Spindle speed	27,850 RPM
Feed per revolution	0.25 mm/rev
Depth of cut	9.96 mm
Widths of cut	16 and 5.94 mm
Machining direction	− 75°, − 60°, − 45°, − 30°, − 15°, 0°, 15°, 30°, 45°, 60°, 75°, 90°

All the experiments were carried out with external and internal water-based coolant, and industrial HSM cutting conditions were used, as defined in Table 2.

4.3 Results of the investigation

The specific cutting coefficients of the piecewise model have been identified by matrix inversion (Eq. 12) and based on the feed forces F_f and normal forces F_n of the n_{cut} =24 cuts of the experiments. Results are illustrated in Fig. 6.

Experimental results show that the mean value of tangential specific cutting coefficient is 1050 MPa and mean radial coefficient is 2360 MPa. Moreover, it is shown that fibres orientation significantly affects the specific cutting coefficients, and consequently on cutting forces. Indeed, variations around the average values are important. Tangential coefficient varies from 80 to 1780 MPa and radial coefficient varies from 780 to 3680 MPa. That is why considering the fibres orientation in cutting force model is necessary.

However, a constant piecewise model is not robust and could lead to different shapes after identifications in relation to the noise in the experimental results. Consequently, based on the observations with the piecewise model, a simplified analytical model is proposed to describe the evolution of the specific cutting coefficients in relation to fibres orientation.

4.4 Specific cutting coefficients model

Due to the previous results (Fig. 6), an analytical model of the specific cutting coefficients in relation to fibres orientation is proposed:

$$\begin{aligned} K_t(\theta) &= K_{tm} + K_{ta} \cdot \sin(2 \cdot \theta + \psi_t) \\ K_r(\theta) &= K_{rm} + K_{ra} \cdot \sin(2 \cdot \theta + \psi_r) \end{aligned} \tag{14}$$

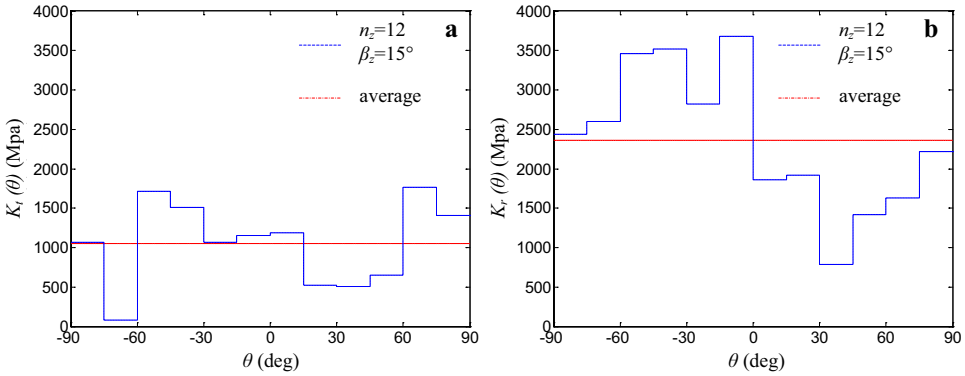

Fig. 6 Evolution of the specific cutting coefficients. **a** Kt(θ) and **b** Kr(θ) identified through a piecewise constant model

where K_{tm} and K_{rm} are the mean values, K_{ta} and K_{ra} their amplitude and ψ_t and ψ_r their phase angle. In accordance with previous investigation, a 2θ appears since θ is π-periodic. Finally, the expressions of cutting forces (11) can be expressed as:

$$\begin{bmatrix} F_f \\ F_n \end{bmatrix} = \frac{f}{2\cdot\pi}\cdot\sum_{i=1}^{m} n_{\psi_i}\cdot e_i\cdot\int_{\chi*}^{\pi}\sin(\chi)\cdot\begin{bmatrix}\cos\chi & \sin\chi\\ -\sin\chi & \cos\chi\end{bmatrix}\cdot\begin{bmatrix}K_{tm}+K_{ta}.\sin(2.\theta+\psi_t)\\ K_{rm}+K_{ra}.\sin(2.\theta+\psi_r)\end{bmatrix}\cdot d\chi \quad (15)$$

In order to simplify the identification of model parameters, the model can be linearized:

$$\begin{aligned} K_t(\theta) &= a_0 + a_1\cdot\sin(2\cdot\theta) + a_2\cdot\cos(2\cdot\theta)\\ K_r(\theta) &= b_0 + b_1\cdot\sin(2\cdot\theta) + b_2\cdot\cos(2\cdot\theta)\end{aligned} \quad (16)$$

$$with \begin{vmatrix} a_0 = K_{tm}\\ a_1 = K_{ta}\cdot\cos(\psi_t)\\ a_2 = K_{ta}\cdot\sin(\psi_t)\end{vmatrix} \quad and \quad \begin{vmatrix} b_0 = K_{rm}\\ b_1 = K_{ra}\cdot\cos(\psi_r)\\ b_2 = K_{ra}\cdot\sin(\psi_r)\end{vmatrix} \quad (17)$$

Thus, Eq. [15] can be expressed as a linear combination of the parameters of specific cutting coefficient model:

$$\begin{aligned} F_f = \frac{f}{2\cdot\pi}\cdot\sum_{i=1}^{m} n_{\psi i}\cdot e_i\cdot\Bigg(&a_o\cdot\int_{\chi*}^{\pi}\sin(\chi)\cdot\cos(\chi)\cdot d\chi + a_1\cdot\int_{\chi*}^{\pi}\sin(\chi)\cdot\cos(\chi)\cdot\sin(2\cdot\theta)\cdot d\chi\\ &+ a_2\cdot\int_{\chi*}^{\pi}\sin(\chi)\cdot\cos(\chi)\cdot\cos(2\cdot\theta)\cdot d\chi + b_o\cdot\int_{\chi*}^{\pi}\sin^2(\chi)\cdot d\chi\\ &+ b_1\cdot\int_{\chi*}^{\pi}\sin^2(\chi)\cdot\sin(2\cdot\theta)\cdot d\chi + b_2\cdot\int_{\chi*}^{\pi}\sin^2(\chi)\cdot\cos(2\cdot\theta)\cdot d\chi\Bigg)\end{aligned} \quad (18)$$

It can be expressed as a matrix product:

$$F_{2n_{cut},1} = A_{2n_{cut},6}\cdot K_{6,1} \quad (19)$$

with F is the matrix containing the experimental cutting forces of the n_{cut} experiments, A the matrix representing chip sections, and K the matrix containing the specific cutting coefficients (a_0,a_1,a_2,b_0,b_1,b_2). These parameters of the analytical model can hence be identified by matrix inversion (Eq. 19).

5 Results

All the experiments presented in Table 2, i.e. 24 couples of feed/normal forces, have been considered in order to identify the parameters of the specific cutting coefficients model (Eq. 14) through matrix system inversion (Eq. 19). Results are presented in Table 3 and illustrated in Fig. 7.

Maximum tangential and radial specific cutting coefficients are obtained respectively for a fibre orientation of −54° and −40° whereas their minimum corresponds to an orientation of 36° and 50°.

Considering the identified model of specific cutting coefficient, feed and normal forces have been calculated (Eq. 15). Simulated cutting forces are compared with experiments in Fig. 8.

The prediction of feed and normal forces is in accordance with the experimental data. The relative errors are respectively estimated at ± 7.8% and ± 5.8% (or ± 39 N and ± 24 N) for machining operation with a low width of

Table 3 Identified parameters of the specific cutting coefficient model

K_{tm}	1053.7 MPa	K_{rm}	2361.5 MPa
K_{ta}	189.8 MPa	K_{ra}	1082.2 MPa
ψ_t	17.3°	ψ_r	− 9°

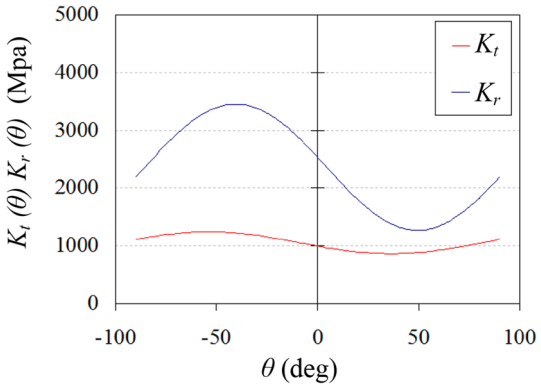

Fig. 7 Analytical model of the specific cutting coefficients in relation to fibre orientation, **a** Kt(θ) and **b** Kr(θ), identified from the experiments

cut (5.94 mm) whereas they are evaluated at ± 3.2% and ± 6.1% (± 46 N and ± 39 N) for a 16 mm tool engagement.

6 Discussion

First point of discussion concerns the levels of specific cutting coefficients. During machining with diamond abrasive cutters, and contrary to machining with endmills, the radial component is more important than the tangential one (Fig. 7). Tool geometry explains this trend. Indeed, rake angles are generally positive for milling with carbide or PCD tools (from 0 to 18°) [2, 19]. Consequently, cutting configuration is favourable and specific cutting coefficients associated to the couple Tool/Material are low. During machining operation with diamond abrasive cutters, cutting is less efficient. Indeed, the rake angles are highly negatives because grits have rather a spherical shape. By tool scanning, Boudelier et al. [4] established that the average rake angle is -65° (Fig. 9). Consequently, level of specific cutting coefficients is higher.

In order to explain the influence of fibres orientation on the variations of specific cutting coefficients, results have been transposed to an orthogonal cutting configuration (Fig. 10). The grit is represented with the average rake angle. A chip section of 1 mm^2 has been considered (f=0.1 mm/rev, a_p=10 mm). Tangential F_t, radial F_r and resultant F_{res} forces have been simulated depending on fibres orientation, using the previously identified parameters (Table 3). Then, the resultant force F_{res} have been projected onto the fibres reference system (x_{fib}; y_{fib}). Two components are obtained: F_{axi} oriented in the fibres direction and F_{trans} orthogonal to the fibres (Fig. 10). Results are shown in the Fig. 11.

Firstly, the lowest resultant force is obtained for a fibers orientation of about 60°. In that case, the grit cutting face is nearly perpendicular to fibres axis (Fig. 10a). Transverse force F_{trans} is negligible and only an axial force F_{axi} is generated

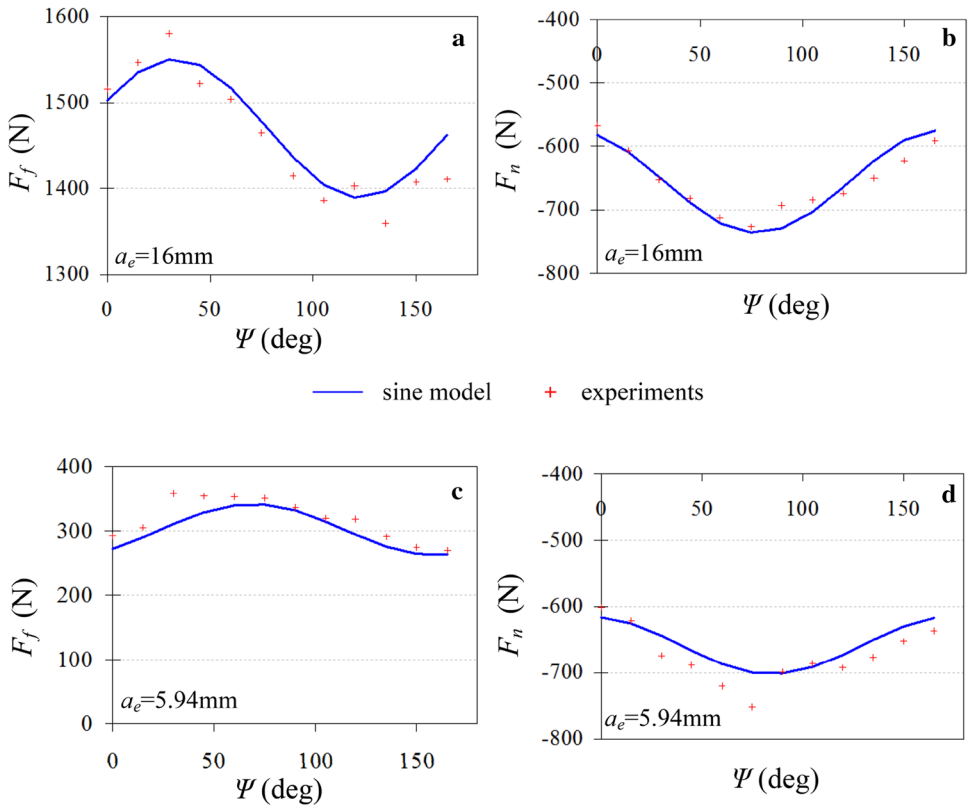

Fig. 8 Experimental and simulated feed forces F_f (**a**–**c**) and normal forces F_n (**b**–**d**), a_e = 16 mm (**a**–**b**) and a_e = 5.94 mm (**c**–**d**)

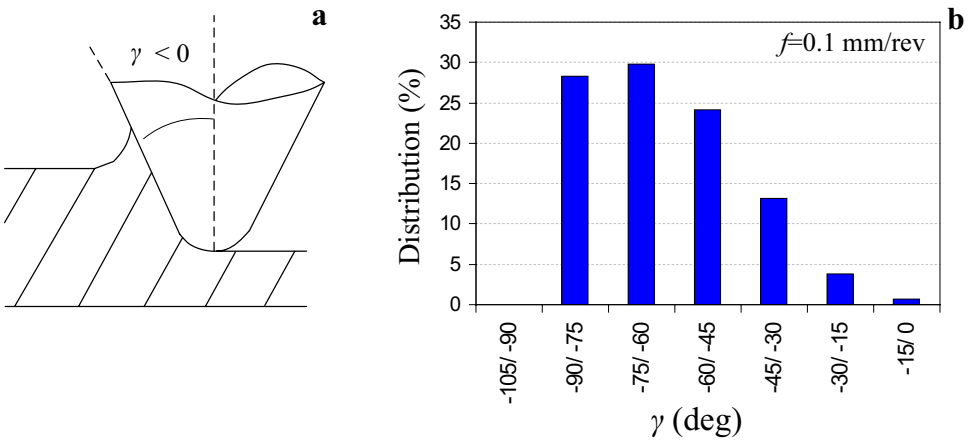

Fig. 9 **a** Definition of grits rake angle, **b** Distribution of grits rake angle on a diamond abrasive cutter (grits size of 852 µm)

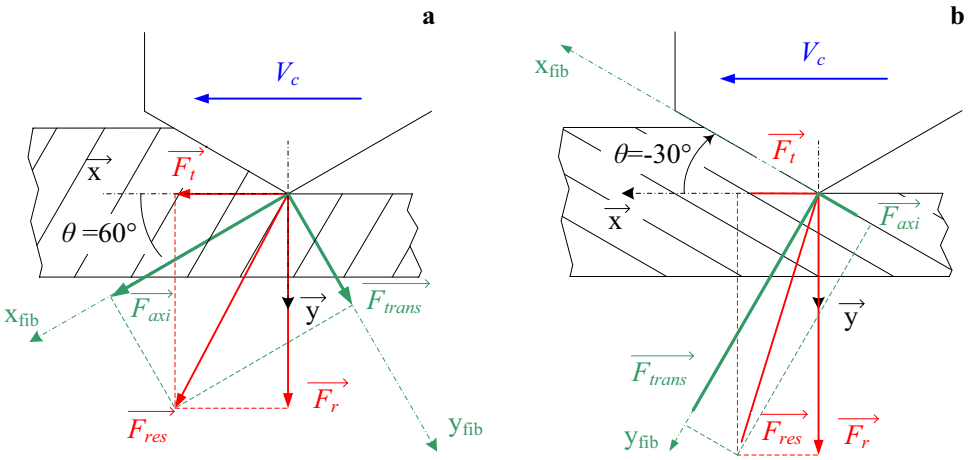

Fig. 10 Cutting forces projection onto fibres reference system

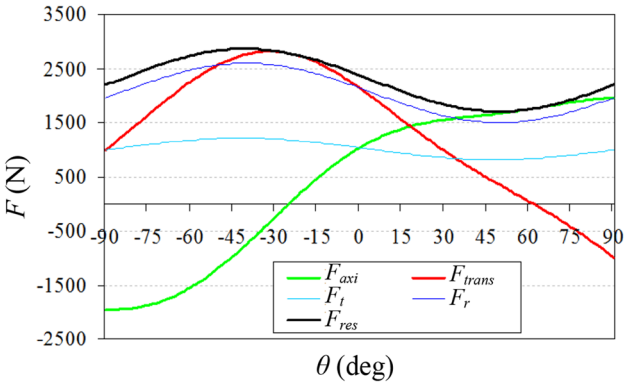

Fig. 11 Cutting forces in orthogonal cutting configuration

(Fig. 11). A compressive load is applied along fibres direction and a significant shear at the fibre–matrix interface appears. It is very favourable to crack initiation and propagation. Indeed, the fibre–matrix interface is considered as the weak point of polymer matrix composites due to their low interlaminar shear strength [17]. As resultant force is minimal, this configuration of fibres orientation is optimum for cutting operation.

The highest resultant force is obtained for fibres orientation around −30°. In that case, the grit cutting face is nearly parallel to fibres axis (Fig. 10b). In this configuration, a significant transverse force F_{trans} is generated, perpendicularly to the grit cutting face. Fibers are compressed the one on the other. Besides, axial force F_{axi} applied on fibres is very low. That leads to very low shear at the fibre–matrix interface. As the weakness of the material is lowly solicited, this configuration is unfavorable for the cut.

7 Conclusions

A cutting force model dedicated to the machining of multidirectional CFRP laminate with diamond abrasive cutters was proposed. The analytical approach is based on the variation of specific cutting coefficients depending on fibres orientation. The following conclusions can be drawn:

1. The model allows accurate prediction of cutting forces during trimming of multidirectional CFRP with diamond abrasive tools, over the entire range of fibres ori-

entation (− 90° to + 90°) and for different widths of cut. Indeed, the simulated forces were in good agreement with the experimental results. Model error was evaluated at ± 7.8% for feed force and ± 5.8% for normal force.

2. An original approach was proposed in order to consider the large number of grits that are randomly distributed around the tool. Conversely to the local engagement of endmill cutting edge, a continuous engagement of the tool was introduced. Coherence with endmill model was verified. This approach represents a significant improvement over previous models and could be extended to grinding applications.
3. Variations of specific cutting coefficients depending on fibres orientation were investigated using a piecewise constant model. It led to the proposal of a sine model for the specific cutting coefficients. Combined with a mixture approach, accurate prediction of cutting forces during trimming operation of multidirectional laminate was obtained.
4. Results of the model were transposed to an orthogonal cutting operation and cutting forces were expressed in the fibres reference system. Cutting mechanisms were then discussed depending on fibres orientation in order to explain the variation of specific cutting coefficients.

Acknowledgements This work was carried out within the context of the working group Manufacturing'21 which gathers 16 French research laboratories. The topics approached are: modelling of the manufacturing processes, virtual machining, and emergence of new manufacturing methods.

References

1. Arola D, Sultan MB, Ramulu M (2002) Finite element modeling of edge trimming fiber reinforced plastics. J Manufac Sc Eng Trans ASME 124(1):32–41
2. Bhatnagar N, Ramakrishnan N, Kaik NK, Komanduri R (1995) On the machining of fiber reinforced plastic (FRP) composite laminates. Int J Mach Tools Manuf 35(5):701–716
3. Bonnet C, Benmohammed B, Poulachon G, Rech J, Girard Y (2011) CFRP drilling model: fiber orientation influence on mechanical load and delamination. Adv Mater Res 223:111–121
4. Boudelier A, Ritou M, Garnier S, Furet B (2011) Optimisation of process parameters in cfrp machining with diamond abrasive cutters. Adv Mater Res 223: 774–783. https://doi.org/10.4028/www.scientific.net/AMR.223.774
5. Boudelier A, Ritou M, Garnier S, Furet B. (2013) Investigation of CFRP machining with diamond abrasive cutters. Revue des Composites et des Matériaux Avancés 23(3):425–436. https://doi.org/10.3166/RCMA.23.425-436
6. Collingan K, Ramulu M (1999) Edge trimming of graphite/epoxy with diamond abrasive cutters. J Manuf Sci Eng 121:647–655. https://doi.org/10.1115/1.2833089
7. Dumas C, Boudelier A, Caro S, Garnier S, Ritou M, Furet B (2011) Development of a robotic cell for trimming of composite parts. Mech Indus 12(6):487–494. https://doi.org/10.1051/meca/2011103
8. Karpat Y, Bahtiyar O, Deger B (2012) Mechanistic force modelling for milling of unidirectionnal carbon fiber reinforced polymer laminates. Int J Mach Tools Manuf 56:79–93. https://doi.org/10.1016/j.ijmachtools.2012.01.001
9. Malkin SK (1989) Grinding technology: theory and applications of machining with abrasives. Ellis Horwood Limited, Chister
10. Nayak D, Bhatnagar N, Mahajan P (2005) Machining studies of UD-GFRP composites part 2: finite element analysis. Mach Sci Technol 9(4):503–528
11. Puw HY, Hocheng H (1998) Chip formation model of cutting fiber-reinforced plastics perpendicular to fiber axis. Trans ASME 120:104–114
12. Ramulu M (1997) Machining and surface integrity of fibre-reinforced plastic composites. Sadhana 22(3):449–472
13. Ramkumar J, Malhotra SK, Krishnamurthy R (2004) Effect of workpiece vibration on drilling of GFRP laminates. J Mater Process Technol 152:329–332
14. Venu Gopala Rao G, Mahajan P, Bhatnagar N (2008) Three-dimensional macro-mechanical finite element model for machining of unidirectional-fiber reinforced polymer composites. Mater Sci Eng 498:142–149
15. Mohamed Slamani S, Gauthier J-F, Chatelain (2015) A study of the combined effects of machining parameters on cutting force components during high speed robotic trimming of CFRPs. Measurement 59:268–283. https://doi.org/10.1016/j.measurement.2014.09.052
16. Sheikh-Ahmad J, Tworney J, Kalla D, Lodhia P (2007) Multiple regression and committee neural network force predition models in milling FRP. Mach Sci Technol 11(3):391–412
17. Sheikh-Ahmad J (2009) Machining of polymer composites, Springer, New York
18. Teti R (2002) Machining of composite materials. CIRP Ann Manufac Technol 51:611–634
19. Wang DH, Ramulu M, Arola D (1995) Orthogonal cutting mechanisms of graphite/epoxy composite. Part I: unidirectional laminate. Int J Mach Tools Manuf 35:1623–1638
20. Wang DH, Ramulu M, Arola D (1995) Orthogonal cutting mechanisms of graphite/epoxy composite. Part II: multi-directional laminate. Int J Mach Tools Manuf 35(12):1639–1648
21. Yuan S, Zhang C, Amin M, Fan H, Liu M (2015) Development of a cutting force prediction model based on brittle fracture for carbon fiber reinforced polymers for rotary ultrasonic drilling. Int J Adv Manuf Technol. https://doi.org/10.1007/s00170-015-7269-x
22. Zhang LC, Zhang HJ, Xiang XM (2001) A force prediction model for cutting unidirectional fibre-reinforced plastics. Mach Sci Technol 5(3):293–305